Quantifying the Urban Heat Island Effects and Energy Performance of Solar-Reflective Facades: A Simulation Study in a Dense Urban Context

Chenshun Chen
Department of Architecture Engineering
Pennsylvania State University
email: cjc7032@psu.edu

Qiuhua Duan Department of Civil, Construction and Environmental Engineering The University of Alabama email: gduan@ua.edu

Enhe Zhang
Department of Architecture Engineering
Pennsylvania State University
email: ekz5068@psu.edu

Julian Wang*
Department of Architecture Engineering
Pennsylvania State University
email: julian.wang@psu.edu

* Corresponding author

ABSTRACT

Many researchers have studied the roles of building envelope materials on UHI, such as roofs, and walls, but few of them have explored the impacts of the emergence of the solar-reflective coatings, films, and panels but well-visible transmittance that is increasingly applied to glazed building facades, especially in hot climates, for outdoor thermal environments. The question then arises: Despite the positive effects of these strong solar-reflective facades on building heating and cooling energy savings, do they have the same positive effects on the adjacent outdoor area, especially in a dense urban context? This research aims to quantify the potential UHI effects of the solar-reflective facades relative to the non-reflective ones in a dense urban context, along with the heating and cooling energy performance analysis. As such, a simulation method in terms of a series of tools including LBNL Radiance, EnergyPlus, and WINDOW software was adopted in this work to analyze the solar radiation interactions between the façade surface and the surrounding urban structures and potential temperature rise under solar-reflective and nonreflective facades. The result shows that the annual cooling energy savings by using the solar-reflective facades are about 33.8% relative to the typical double-pane clear glazed façade because of the substantial reduction of U-factor and solar heat gains; But, this preliminary work also unveils the potential adverse effects of using such materials at the urban scale, leading nearly 2 times greater solar irradiation and UHI effects than the ones by the solar-non-reflective building surfaces in an urban area. Future optimization studies on the trade-off between the building cooling energy savings and UHI effects by the solar-reflective façades need to be conducted.

KEYWORDS

Solar-reflective façade, Urban heat island, Building façades, Simulation, Solar radiation

INTRODUCTION

Urban Heat Island (UHI) effect is defined as the rise in temperature in any man-made area, which results in a well-defined, distinct "warm island" of urban area among the surrounding natural landscape [1]. The adverse effects of UHI include degradation of the living environment, increase in energy consumption, elevation in ground-level ozone, and even an increase in mortality rates [2]. Two major sources induce the temperature increase in an urban area: one is solar irradiation, including direct sunlight exposure and indirect energy from re-directed and absorbed solar radiations by urban structures; the other one is anthropogenic heat, which is produced by population-related activities and air pollutants. However, despite the large amount of heat produced by building structures in the urban microclimate, designers and engineers still put a lot of effort into designing solar-reflective facades to enhance building energy efficiency and indoor thermal comfort, especially in cooling-dominated climates. For example, most Low-E coatings used for fenestration systems, especially those with low solar heat gain coefficient (SHGC) for hot climates, are solar-reflective, which transmits the most visible light but reflects a large portion of solar infrared radiation (heat). The global market for Low-E Glass estimated at US\$45.3 Billion in the year 2020, is projected to reach a revised size of US\$88 Billion by 2027 [3]. Other technologies include NIR-selective coatings for envelopes [Error! Reference source not found.], cooling pavements and roofs [4], metal panels, etc. As these types of materials become more popular, their impact on the urban microclimates draws the increasing attention of researchers: Synnefa et al. compared 14 types of reflective coatings and found that by the use of reflective coatings on white concrete tile' surface, its surface temperature could reduce 4 °C during a hot summer day and 2 °C during hot summer night [6]. Yuan et al. used the Computational Fluid Dynamics (CFD) analysis method to predict outdoor thermal comfort by using diffuse HR building coating and specular reflective building coating. A total of three thermal sensation indices including outdoor air temperature (Ta), wet bulb globe temperature (WBGT), and new standard effective temperature (SET*) with consideration of the outdoor solar radiation effect are used to evaluate the outdoor thermal comfort under diffuse and specular reflective building coatings [7]. Yoshida et al. compare the effects of a heat ray retro-reflective film and other countermeasure techniques for windows, from the perspective of reducing the cooling load and mitigating the effects on the thermal environment. It is found that retro-reflective film improves both indoor and outdoor thermal environments; however, Low-E coatings improve indoor thermal

conditions but possibly worsen outdoor thermal environments [8]. Although these prior studies have explored the impacts of some reflective materials on UHI, one fundamental research question is still not answered yet – *compared to the non-solar-reflective façade*, whether and to what extent the solar-reflective façade (i.e., low SHGC Low-E glazing) contributes to UHI.

In brief, the solar-reflective façade may enhance the indoor thermal environment and reduce the building cooling loads in summer, while it also has a high potential to worsen UHI which may in turn affect outdoor microclimate and return the negative effects on the buildings and their occupants. Before addressing and analyzing such trade-off issues (building energy savings vs. UHI), it is necessary to quantify the UHI differences between the facades with and without solar-reflective features. In particular, with the increasing development and applications of NIR-reflective coatings, films, and panels for building façades toward building energy efficiency, such technologies' impacts on UHI need to be taken into account during the decision-making process.

METHODOLOGY

Step 1 – Creating glazing models.

A comparative study was conducted in this work to understand the effects of solar-reflective materials (i.e., Low-E coating) on windows to UHI intensity. Two models were built in LBNL Optics: The design model (Model I) is a Double-Pane Low-E window, made by ipasol platin 25/17 6mm Clearvision + Air (5%)/Argon (95%) gap + Generic Clear 6mm Glass, with Low E coating on the back of layer 2 (E2=0.025). The baseline model (Model II) is a Double-Pane clear window, consisting of Generic Clear 6mm Glass + Air (5%)/Argon (95%) gap + Generic Clear 6mm Glass. Figure 1 shows the spectral transmittance and reflectance (back and front) properties of the two glazing models, Model I has around 20% solar transmittance in the visible region but very low transmittance in the NIR region. On the other hand, its solar reflectance exceeds 60% when beyond the UV region. The baseline model, however, has a high visible transmittance but low front solar reflectance. Detailed glazing properties of these two models are shown in Table 1. The selection of these two models was to mimic two typical scenarios – poorly-insulated glazing with minor solar reflection and highly-insulated glazing with strong solar reflection. It should be noticed that even though glazing systems' spectral properties are provided, these models calculate the average visible/solar transmittance and reflectance by referencing ASTM G173-03 solar spectral irradiance function [12] so that simulations are spectrally independent. Also, notably, the BRDF function (reflectance distribution of glazing surfaces) derived from the LBNL Optics program could be incorporated into the raytracing process in solar radiation analysis, but in this work, we just assume all the glazing systems are specular-reflected, thus, all the simulations are also angularly independent.

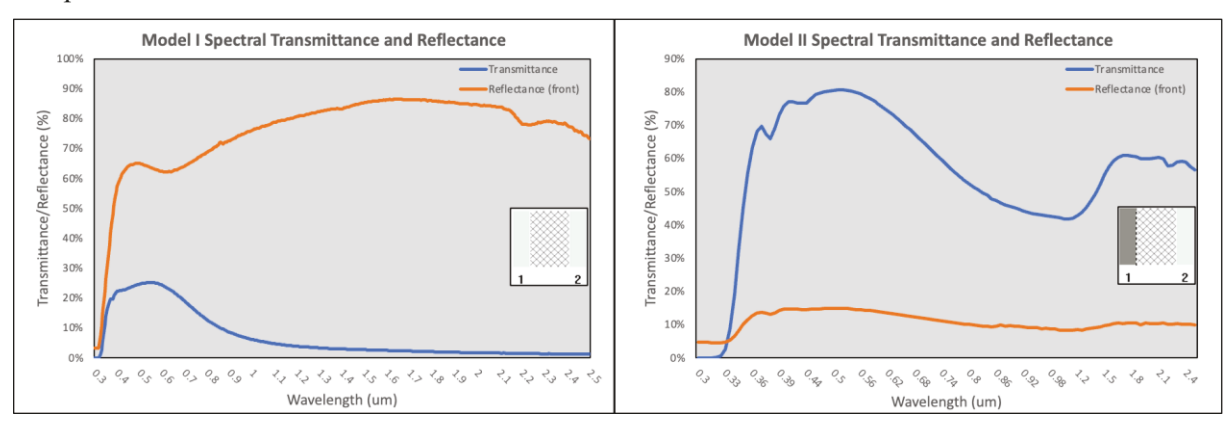


Figure 1. Glazing system spectral properties (300nm to 2500nm)

Table 1. Glazing system properties used in the simulation

Model	Tvis	R _{fvis}	Tsol	\mathbf{R}_{fsol}	Abs1	Abs2	U-factor (W/m ² K)	SHGC
I	0.2468	0.6317	0.1418	0.6947	0.1436	0.0199	1.350	0.168
II	0.7811	0.1422	0.6069	0.1137	0.1684	0.1124	2.539	0.604

Step 2 – Building an urban model.

A local-scale (microscale) urban model was built using Elk (a Grasshopper plugin), which depicts topographies and street maps using data from OpenStreetMap.org and Shuttle Radar Topography Mission (SRTM) data from NASA/Jet Propulsion Laboratory [10]. The urban model has a map area of 392m × 312m (121,604m2), ranges from (39.95901° N, 39.95261° S), (-75.17782° W, -75.16536° E. As shown in Figure 2, the urban model contains buildings, streets, sidewalks, and leisure/open information in the Logan Square area, Philadelphia.



Figure 2. The urban model of Logan Square, Central Philadelphia (Left: Snapshot of Logan Square, Philadelphia from Google Earth; Right: Top & Perspective view of Rhino 3D model)

All high-rise buildings were transformed into Dragonfly (DF)-Building components, with a uniform story height of 8m (which is unrealistic but would help reduce the computational load). Then this DF model was converted to Honeybee (HB) model, within which each story represents an HB-Room component. Apertures were then assigned to these HB-Rooms, with a uniform Window-Wall Ratio (WWR) of 80% (except for context buildings). HB-Ground rooms were also created in segments (meshlike) to increase the spatial distribution accuracy, and the ground materials were downsized to three major types: asphalt, concrete and grassy lawn, to mimic different ground areas. However, some features of this urban model are either missing or simplified. For example, the building blocks are simply extruded as boxes without any complex shapes; ground zones have been pruned to have only three types, leisure areas, sidewalks, and roads; vegetation in the urban area has been neglected, which might have a large impact on the simulation results since vegetation can help to mitigate UHI effect. After all these steps, the HB model was ready for energy and radiance simulations, which could help to quantify the UHI effect from various perspectives. Figure 3 shows the rendering view of the complete HB model.

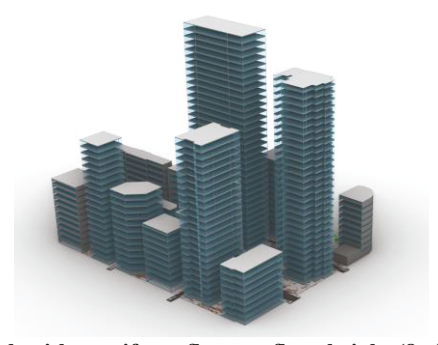


Figure 3. HB model, with a uniform floor-to-floor height (8m) and WWR (80%)

Step 3 – Indoor building energy simulation.

The first step in our study is to conform the building energy reduction by using high solar-reflective facades (for example, Low-E windows), especially cutting down on cooling energy during hot summer days. To perform a district-level urban energy simulation, we utilized URBANOpt (or Urban Renewable Building And Neighborhood Optimization) platform developed by the National Renewable Energy Laboratory (NREL). By integrating with other simulation tools, such as EnergyPlus and OpenStudio, URBANopt offers detailed building energy modeling and analysis. Its flexibility allows users to assess different combinations of building materials, constructions, and systems, as well as district-level energy infrastructure, such as district heating and cooling networks or microgrids. Honeybee and Dragonfly toolkits in Rhino were used to build up the URBANOpt simulation. The detailed workflow schema is shown in Figure 4 [11].

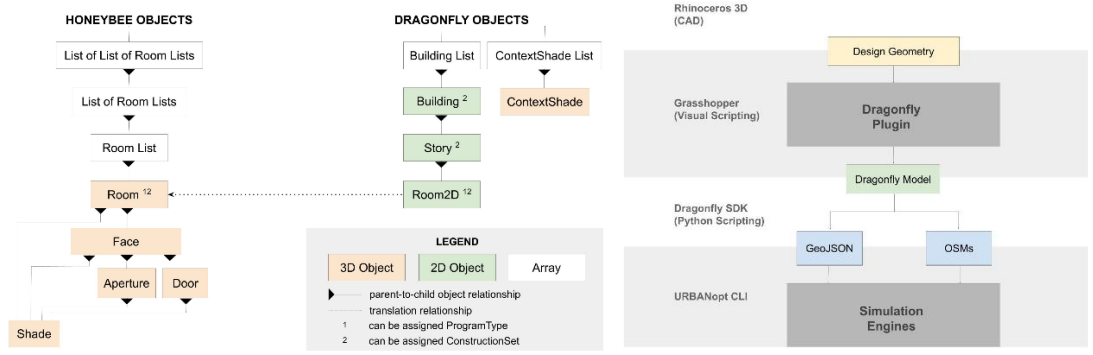


Figure 4. Integration of Rhino Honeybee/Dragonfly with URBANOpt

Firstly, Dragonfly building objects were created from the urban model, with a fictional story height of 8m and a window-wall ratio of 80%. Then these Dragonfly objects were converted to Honeybee objects to change window constructions in order to compare the building energy simulation results, such as energy use intensity, total energy consumption, etc. All the other construction materials were set according to Climatezone 5 building templates, with detailed information shown in Table 2. 'Large-office' was assigned as the building program. All the buildings were conditioned, with 'Ideal Loads Air System' as an HVAC template [12].

Construction	Materials	U-Value (W/m2-K)	Heat capcacity (J/K-m²)	Thickness (m)	SHGC	VT
Window	Double Low-E (Model I)	1.82	-	0.02	0.11	0.08
Willdow	Double Clear (Model II)	4.49	-	0.02	0.69	0.60
Exterior Wall	'Generic Brick', 'Generic LW Concrete', 'Generic 50mm Insulation', 'Generic Wall Air Gap', 'Generic Gypsum Board'	0.46	273003.9	0.36	-	-
Ground Slab	'Generic 50mm Insulation', 'Generic HW Concrete'	0.57	405801.5	0.25	-	-
Interior Ceiling	'Generic LW Concrete', 'Generic Ceiling Air Gap', 'Generic Acoustic Tile'	1.42	111990.4	0.22	-	-
Interior Floor	'Generic Acoustic Tile', 'Generic Ceiling Air Gap', 'Generic LW Concrete'	1.42	111990.4	0.22	-	-
Roof	'Generic Roof Membrane', 'Generic 50mm Insulation', 'Generic LW Concrete', 'Generic Ceiling Air Gap', 'Generic Acoustic Tile'	0.41	130943.9	0.28	-	-

Table 2. Detailed HB-Energy Model Construction sets

Step 4 – Outdoor radiation simulation.

To compare the impacts of different solar-reflective facades on urban heat island, the first step is to understand how solar reflectance of building facades affect the outdoor ground horizontal irradiance (GHI). As in urban areas, a large portion of the solar irradiance received by a ground surface would not directly come from the sun, but re-directed or re-radiated by its surrounding surfaces, especially in city-intensive areas. In this study, Honeybee Point-In-Time Grid-Based recipe was used (which utilizes Radiance as the embedded engine) to generate an outdoor GHI heatmap. Building window materials are modified by Radiance Glass Modifiers (integrating BRTD functions), as shown in Figure 5, in which only transmitted and reflected rays in the mirror direction will be considered.



Figure 5. Radiance Glass BRTD modifier

It should be noticed that Radiance divides the light source and materials' properties into red, green, and blue channels in its simulation process, in other words, radiance modifiers only contain RGB transmittance/reflectance values which are derived from the spectral properties of the glazing material by integrating over the visible spectrum and converting to RGB values. Detailed solar spectral transmittance/reflectance can be obtained from the IGDB database, but in this study, we just assume these to be constant across the whole solar spectrum (i.e., RGB transmittance/reflectance are all equal to T_{sol} and R_{fsol} listed in Table 1). As for the analysis period, we chose an extreme cooling hour, at 12:00 PM, August 4^{th} , with clear-sky conditions (GHI equals 844 W/m² and DNI equals 544 W/m², according to Philadelphia_International_Ap:: 724080:: TMY3 file). The analysis points were generated at the surface of the ground, with a grid size of 3.0×3.0 m. The general simulation procedure is illustrated by the diagram in Figure 6, with the Radiance parameters set as the following:

Parameter **Abbreviation Definition** Values This value will approximately equal the error from indirect illuminance interpolation. Positive values between 0 and 1 control the allowed error for **Ambient** 0.2 -aa interpolation. Lower values result in higher accuracy accuracy, while higher values allow for more error in exchange for faster computation times. This parameter controls the number of indirect **Ambient** light bounces considered in the simulation. A 6 -ab **bounces** higher value results in a more accurate simulation but at the cost of increased computation time. This parameter sets the distance between ambient calculations by determining the maximum density **Ambient** of ambient values used in interpolation. Higher 64 -ar resolution values provide finer grids and better accuracy, but increased computation time. This parameter sets the number of initial sampling rays sent from each ambient point into the **Ambient** hemisphere to determine the indirect incident light. 2048 -ad divisions A higher value improves the accuracy of indirect lighting but increases the computation time.

Table 3. Radiance simulation parameters

Ambient		The number of extra rays that will be used to	
super-	-as	sample areas in the divided hemisphere that appear	2048
samples		to have high variance.	

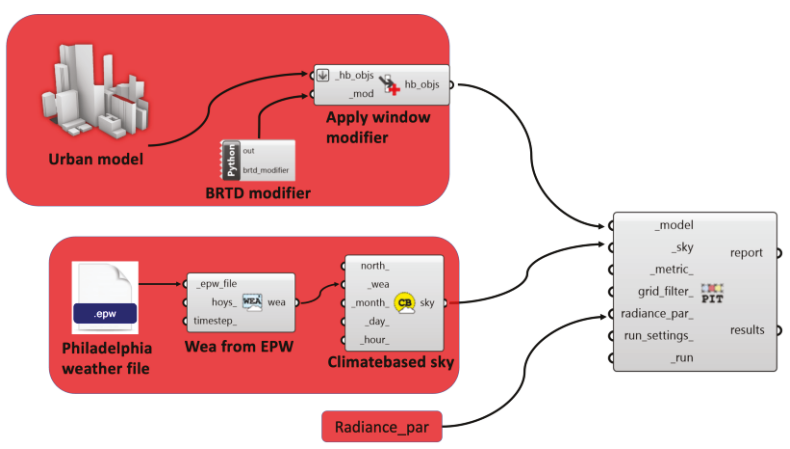


Figure 6. HB-Radiance scheme of generating ground solar irradiance

In addition to the previously discussed work, we also conducted a sky-view factor (SVF) analysis to find the percentage of the sky dome seen by each grid point, as shown in Figure 7. This contributed to a better understanding of the degree of obstruction by the building contexts for each analysis point and helped us to find the locations that were most likely affected by their adjacent solar-reflective facades.

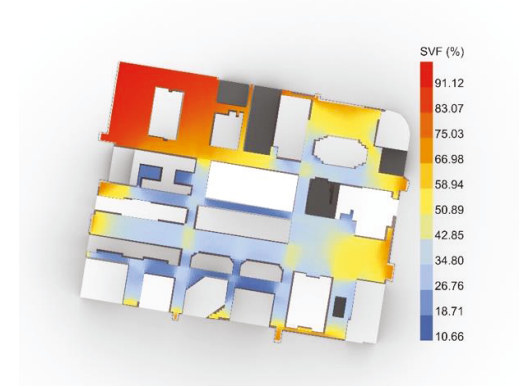


Figure 7. Sky view factor map

Step 5 – Outdoor ground temperature simulation.

Another important scaling factor of the UHI effect is the surface temperature, as it directly represents the amount of heat absorbed and re-emitted by urban surfaces, and thus helps us to quantify the UHI intensities from a heat transfer perspective. To get the outdoor ground surface temperature, the Honeybee ModelToOSM component was used to run the EnergyPlus simulation inside the OpenStudio platform. In EnergyPlus, outdoor surface temperatures are calculated using Equation 1, where q''_{asol} is the exterior shortwave radiation; q''_{LWR} is the longwave radiation exchange between the surface, the sky, and the ground; q''_{conv} is the exterior convective heat flux (there is a wide range of selections for determining $h_{c,ext}$, which could be found in EnergyPlus Engineering Reference [13], and will not be introduced in detail here). It is worth mentioning that when calculating the solar reflection reflected from the exterior surfaces, EnergyPlus only considers single-time solar reflection. Therefore, in the process of calculating shortwave solar radiation received by the ground, EnergyPlus may underestimate the value because of the high-density obstructions within the urban model.

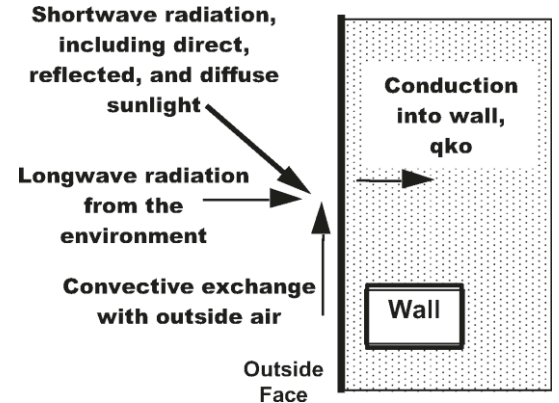


Figure 8. EnergyPlus outside surface heat balance diagram

$$q''_{\alpha sol} + q''_{LWR} + q''_{conv} - q''_{ko} = 0$$

$$q''_{LWR} = h_{r,gnd} (T_{gnd} - T_{surf}) + h_{r,sky} (T_{sky} - T_{surf}) + h_{r,air} (T_{air} - T_{surf})$$

$$Q_c = h_{c,ext} A (T_{surf} - T_{air})$$
(1)

As for the ground materials, their thermal properties would have large impacts on the surface temperature, therefore, we defined three different types of ground materials, and listed their detailed thermal properties in below:

Table 4. Detaile	d ground ma	aterials' the	ermal proper	ties
------------------	-------------	---------------	--------------	------

Surface	Material	Albedo	U-Value (W/m ² -K)	Density (kg/m²)	Heat Capacity (J/K-m ²)
Road	Asphalt	0.13	3.75	472.0	434,240.0
Sidewalk	Concrete	0.35	8.65	448.6	375,478.2
Garden	Grassy lawn	0.22	3.5	110.0	132,000.0

Since EnergyPlus can only produce surface temperature results for rooms/thermal zones, mesh-like segmented 'ground rooms' were created by using the HB-Enegry Ground component in Rhino (there were 2613 'ground rooms' in total). This would help increase the accuracy of the spatial temperature distribution so that hotspots could be spotted but at a cost of high computational-power demand and longer simulation timespan. The basic window constructions' properties used in EnergyPlus simulation are shown in Table 5 (in which solar absorptance ($\alpha = 1 - \tau - \rho$)). The analysis period is the same as the ground irradiation simulation, which is 12:00 PM, August 4th. The general work schema is shown in Figure 9.

Table 5. Detailed EnergyPlus window constructions properties

Model	Solar Transmittance (τ)	Solar Reflectance (ρ)	Solar Absorptance (α)	Front Emissivity
I	0.14	0.70	0.16	0.840
II	0.60	0.07	0.33	0.840

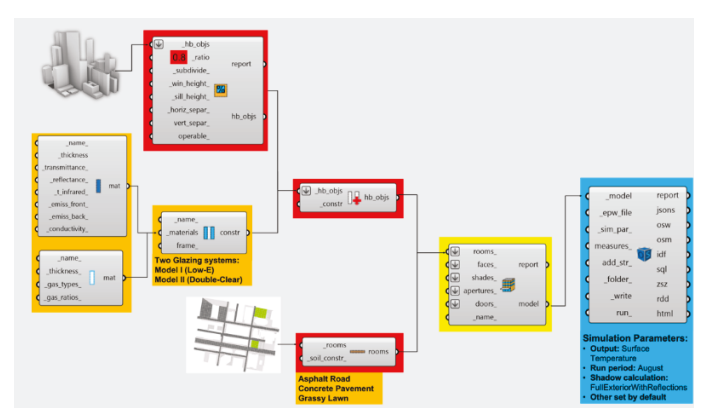


Figure 9. HB-Energy scheme of generating land surface temperature

RESULTS

1) Monthly building energy use

District-level energy use intensity (EUI) and monthly total energy use are shown in Table 6 and Figure 10, respectively. It's found that the heating and cooling energy use will have a great reduction, 68.89kWh/m² vs. 99.97kWh/m², if a Double-Pane solar-reflective Low-E window was applied. In particular, the cooling energy savings can be around 33.8% because of the reduction of both U-factor and solar heat gains in summer. These results demonstrate the capability of Low-E windows on building energy saving on an urban scale. However, their impacts on outdoor thermal environments remain unclear and will be studied and demonstrated in the following sections.

Site EUI	Model I (kWh/m²)	Model II (kWh/m²)
Heating	23.846	31.646
Cooling	45.044	68.325
Sum	68.89	99.97

Table 6. District-level Energy Use Intensity (EUI) for different end users

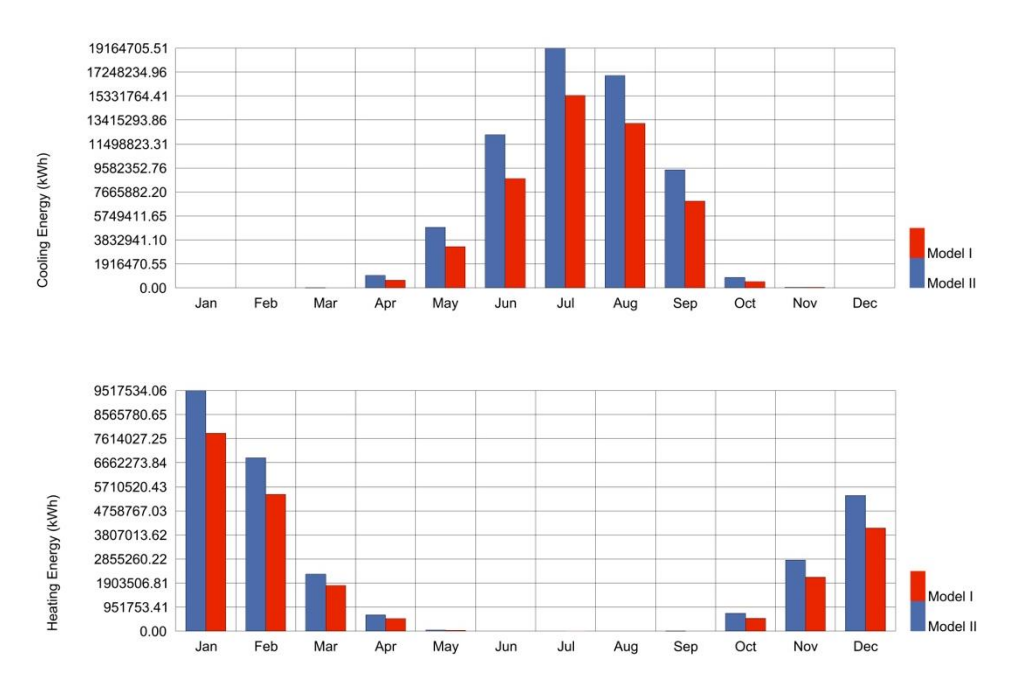


Figure 10. District-level Monthly total energy use (Up: Cooling energy use; Bottom: Heating energy use)

2) Ground solar irradiation

From Table 7, it is known that after applying the Low-E window for the building facades, the maximum and minimum solar irradiance received by the ground surface increased by 9.83%, 162.48%, respectively. The average ground solar irradiance also increase by 17.74%. The ground irradiance spatial heatmap also confirms these results, as shown in Figure 11, the total ground area that has solar irradiance larger than 800 W/m² is 12.2% for Model I but only 3% for Model II. The ground solar distribution heavily depends on SVF and surrounding contexts for each analysis point, but high building density areas are more likely to be affected by high solar-reflective building facades. For example, at the greenmarked point 1, Model I has a ground irradiance of 121.67 W/m², which is 1.06 times larger than that of Model II (59.00 W/m²). Point 2, however, only has a 4.3 % difference between Model I (768.86 W/m²) and Model II (737.13 W/m²). This unveils the effect of re-directed radiation by building surfaces on adjacent ground. Thus, it can be concluded that high solar-reflective building facades will re-radiate more solar radiation to the ground compared to traditional glazing systems.

Table 7. Maximum, Minimum, and Average Ground Solar Irradiance

Model	Maximum Ground Irradiance (W/m²)	Minimum Ground Irradiance (W/m²)	Average Ground Irradiance (W/m²)
I	914.43	91.29	452.88
II	832.59	34.78	384.64

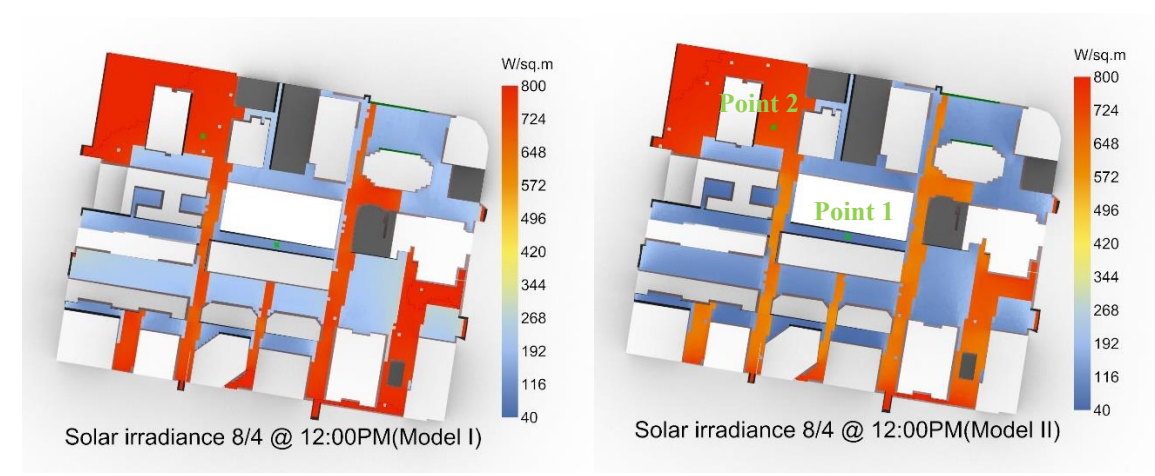


Figure 11. Ground solar irradiation heatmap (Left: Model I; Right: Model II)

3) Ground surface temperature

Table 8 records the maximum, minimum, and average ground surface temperature of the two models. To investigate the extent of temperature variation for different ground materials, three sub-surfaces' (with different ground materials) temperatures are also shown in Table 9. For the entire ground surface, the maximum temperature has a 2.34°C difference between Model I and Model II, while the average temperature has 1.8°C. As for the sampled points of different ground types, asphalt road exhibits the greatest temperature difference, followed by a concrete sidewalk, and grassy lawn's temperature is less affected by its surrounding building facades. The possible reason for these results might be due to the location of the sample points, thus, further analysis may need to be conducted to study the ground typebuilding facades interaction by controlling the sampled points locations. Figure 12 shows the spatial LST heatmap, in which we could spot some 'hotspots' over the entire ground surface. For example, the crossroad area seems to have extremely high temperatures. The general temperature distributions are in accordance with ground irradiation analysis, but there are still some differences between Model I and Model II. For example, in a high-density urban area (circled in red), Model I has higher surface temperatures than Model II for the same locations. To summarize, building facades' solar reflectivity does have an impact on the surface temperature of their surrounding ground, especially in the area of high building density. This difference could be even larger considering EnergyPlus only perform singletime reflection calculation.

Table 8. Maximum, Minimum, and Average Ground Surface Temperature

Model	Maximum Ground Temperature (°C)	Minimum Ground Temperature (°C)	Average Ground Temperature (°C)
I	69.67203	27.4372	40.63303
II	67.33064	27.6499	38.85421

Table 9. Sample Points Temperature for Three Different Ground Types

Mode	Asphalt Road Sample	Concrete Sidewalk	Grassy Lawn Sample
1	Temperature (°C)	Sample Temperature (°C)	Temperature (°C)
I	45.35054	36.373076	44.735624
II	41.581193	33.386597	44.735323

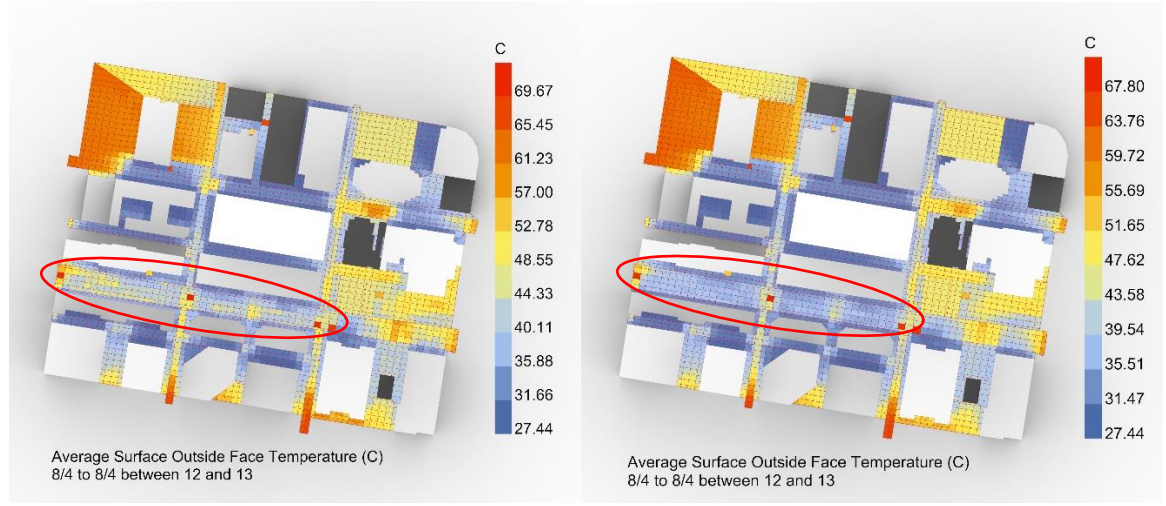


Figure 12. Land Surface Temperature (LST) heatmap (Left: Model I; Right: Model II)

CONCLUSION

This work investigates the impacts of solar-reflective facades on UHI, in the Central Philadelphia area, during the extreme cooling month of the year. To compare the effects of different solar-reflective building facades on UHI, an Rhino 3D model was built by referencing geographical data (mainly contains building and ground surface information) obtained from the Openstreet map, and then transformed into an HB model to run energy and radiance simulations. Two models were compared by only changing the materials of window constructions (i.e., other parameters remain the same as control variables). These two models were made by the generic double-pane clear window and double-pane Low-E window, respectively, to represent building facades' different levels of reflectivity, transmissivity, and emissivity. The positive effects of the Low-E window on building energy saving were confirmed by URBANOpt simulation, in which both cooling and heating energy use was reduced by applying the Low-E window. In order to quantitatively measure the effects of solar-reflective facades on urban thermal environment, two simulation tools were used: the first one utilized the HB-Radiance tool (built upon LBNL Radiance), which calculates the solar irradiance received by the ground surface under a specific weather-based sky condition. By changing the Radiance BRTD modifiers that were assigned to apertures, the correlation between building facades' solar reflectivity and ground surface irradiance can be analyzed. It was found that ground solar irradiance was enhanced by high solarreflective facade, especially in high building density areas. The second simulation utilized the HB-Energy tool (built upon LBNL EnergyPlus), which calculates building exterior surface temperatures by simply implementing the heat balance equations on building exterior surfaces. The results showed that the Low-E window will increase ground surface temperature and induce some 'hotspots', especially in the high-density urban area.

The major contribution of this work is to find the connections between UHI intensity and solar-reflective building facades so that researchers and designers can understand the trade-off between building indoor and outdoor thermal environments by using high solar-reflective windows. This procedure is purely based on computer simulations, so it is highly flexible and can be applied to different scenarios. It shed some light on the glass material development and urban planning, for example, developing retro-reflective glass to reduce the solar energy re-directed by the windows to the urban canyon, adopting counter-measures (such as vegetation) at the 'hotspots' in the urban area to mitigate UHI effect. As more and more buildings have been equipped with glass curtain walls, it is important to control the solar radiation re-radiated by these curtain walls, or they may cause severe climate issues. Despite the contributions this work had made, some research gaps are still waiting to be filled: for example, as spectral-selective window material emerges, it is necessary to consider the spectral dependence of window reflections in building facades-UHI interactions. Also, by considering bidirectional reflection distributions (BRDF) of window materials, it is possible to more accurately locate the 'hotspot' around a solar-reflective building, so that counter-measures could be applied to this area to mitigate the effect.

Furthermore, to validate the simulation results, some field tests could be done by measuring the UHI intensities of different solar-reflective buildings/models.

ACKNOWLEDGMENT

We acknowledge the financial support provided by the U.S. National Science Foundation Fund #2215421: An Integrated Framework to Investigate Thermal Resilience of Sustainable Buildings and Living Environments for Greater Preparedness to Extreme Temperature Events.

NOMENCLATURE

Bidirectional Reflectance Distribution Function
Visible Light Radiation
Near-Infrared Radiation
Global Horizontal Irradiance
Direct Normal Irradiance
Diffuse Horizontal Irradiance
Urban Heat Island
Urban Heat Island Intensity

REFERENCES

- 1. Oke TR. Boundary layer climates. Methuen: University Paperbacks; 1987.
- 2. Rizwan, A. M., Dennis, L. Y., & Chunho, L. I. U. (2008). A review on the generation, determination and mitigation of Urban Heat Island. Journal of environmental sciences, 20(1), 120-128.
- 3. ltd, R. and M. (n.d.). Low-E glass global market trajectory & analytics. Research and Markets Market Research Reports Welcome. Retrieved May 22, 2022
- 4. Zhang, E., Duan, Q., Wang, J., Zhao, Y., & Feng, Y. (2021). Experimental and numerical analysis of the energy performance of building windows with solar NIR-driven plasmonic photothermal effects. *Energy Conversion and Management*, 245, 114594.
- 5. Akbari, H., & Matthews, H. D. (2012). Global cooling updates: Reflective roofs and pavements. Energy and Buildings, 55, 2-6.
- 6. A. Synnefa, M. Santamouris, I. Livada, A study of the thermal performance of reflective coatings for the urban environment, Solar Energy, Volume 80, Issue 8, 2006, Pages 968-981, ISSN 0038-092X, https://doi.org/10.1016/j.solener.2005.08.005.
- 7. Yuan, J., Yamanaka, T., Kobayashi, T., & Kitakaze, H. EVALUATION OF OUTDOOR THERMAL COMFORT UNDER BUILDING EXTERNAL WALL SURFACE MATERIALS WITH DIFFERENT REFLECTIVE DIRECTIONAL CHARACTERISTICS BY CFD.
- 8. Yoshida, S., Yumino, S., Uchida, T., & Mochida, A. (2015). Effect of windows with heat ray retroreflective film on outdoor thermal environment and building cooling load. J. Heat Isl. Inst. Int, 9, 67-72.
- 9. G03 Committee, "Tables for Reference Solar Spectral Irradiances: Direct Normal and Hemispherical on 37 Tilted Surface," ASTM International. doi: 10.1520/G0173-03R20.
- 10. OpenStreetMap contributors. (n.d.). OpenStreetMap. Retrieved [April 25, 2023], from https://www.openstreetmap.org
- 11. Charan, T.; Mackey, C.; Irani, A.; Polly, B.; Ray, S.; Fleming, K.; El Kontar, R.; Moore, N.; Elgindy, T.; Cutler, D.; Roudsari, M.S.; Goldwasser, D. Integration of Open-Source URBANopt and Dragonfly Energy Modeling Capabilities into Practitioner Workflows for District-Scale Planning and Design. Energies 2021, 14, 5931. https://doi.org/10.3390/en14185931
- 12. Big Ladder Software. (2021). Ideal Loads Air System. EnergyPlus Engineering Reference, Version 8.0. Retrieved April 25, 2023, from https://bigladdersoftware.com/epx/docs/8-0/engineering-reference/page-092.html

13. U.S. Department of Energy. (2021). EnergyPlusTM Version 22.1.0 Documentation. Building Technologies Office, Office of Energy Efficiency & Renewable Energy. https://energyplus.net/assets/nrel_custom/pdfs/pdfs v22.1.0/EngineeringReference.pdf